

Synchronous versus asynchronous dynamics in spatially distributed systems

Erik D. Lumer and Grégoire Nicolis

Faculté des Sciences and Center for Nonlinear Phenomena and Complex Systems, Université Libre de Bruxelles, Campus Plaine, C.P. 231, Boulevard du Triomphe, 1050 Bruxelles, Belgium

Received 4 June 1993

Revised manuscript received 4 October 1993

Accepted 6 October 1993

Communicated by F.H. Busse

Many prototypical models of spatially extended systems that are capable of complex spatiotemporal dynamics impose a finite discretization window of space and time. For such models, it is important to determine to what extent the specific procedure which is used to update local states affects the overall regimes, as the latter might turn out to be artifacts due to an unrealistic digitalization of the world. The chances of generating spatiotemporal patterns with no counterparts in the physical world are particularly high with granular space-time models that rely on a synchronous evolution of distributed states, as such synchronous evolution is found in nature most typically in systems governed by evolution laws in the form of partial differential equations. We show this possibility to be the case for the regimes produced in coupled map lattices, as markedly different dynamics arise when the standard synchronous model is made asynchronous. By quantifying the degree of mutual asynchrony in the system, signatures of asynchronous spatiotemporal dynamics are unraveled and further characterized in terms of simple stability measures.

1. Introduction

The complexity of the dynamics of many spatially distributed systems has long hindered the development of systematic quantitative studies. Recent advances, however, have opened the door to detailed probings into the regimes exhibited by a variety of spatially extended systems, from turbulent fluids, to reaction-diffusion processes in chemical reactors, to collective social and biological systems. These advances originate in part from the development of prototypical models of complex systems, which lend themselves to elaborate computer simulations, and for which theories pertaining to low-dimensional dynamics offer the prospect of being extended so as to account for space.

While the relevance of a generic model to the study of a particular phenomenon must be addressed specifically, it is worth considering in broader terms the way in which a model of complex spatiotemporal regimes deals with the continuous space-time structure (at least at the level of a macroscopic approach) of their embedding physical world. Indeed, a common modelling procedure to achieve tractable analysis and efficient computer simulations consists in discretizing some or all of the spatial, temporal, and state variables. For instance, this procedure characterizes the widely used cellular and lattice-gas automata [1,2], in which spatial dimensions are reduced to locations on a cellular grid, and digitalized states are updated at discrete time steps. Likewise, the modelling of spatiotemporal chaos

based on the so-called coupled map lattices relies on a granular space and time, while each site of the lattice is a dynamical system with state variables taking on continuous values [3–5].

One might be tempted to look at such models as discretized versions of the continuous partial differential equations governing the evolution of the underlying system. This view is, in general, unjustified. A discretization of a continuous law - a standard procedure followed in computer simulations - provides a satisfactory picture of the original system only if the time and spatial steps, respectively δt and δr , are sufficiently small. Now, in most cases, interesting behavior in prototype discretized systems is found when δt and/or δr are finite. The question then arises whether such systems can still be regarded as a representation of a certain physical situation, or rather as useful toy models for exploring complicated behavioral patterns in nonlinear dynamics.

When only δt is discrete, the answer is clear: Discrete time dynamics is obtained from a continuous one on a Poincaré surface of section cutting transversally the (continuous) phase-space trajectories [6]. Besides, in the biological arena, it is by now known that discrete time dynamics may describe the relevant part of the evolution of synchronously growing population systems, the step δt representing in this case the generation time. The situation may be quite different when a finite space discretization step δr is in addition imposed in a spatially distributed system. The way in which a discrete time is represented at different spatial locations becomes an issue, for a strong dependence of dynamical regimes on the specific model of time being used has been noticed in a number of studies, whether in relation with Monte Carlo simulations of physical and chemical systems [7,8], or in automata-like abstractions of social and biological processes [9,10,12]. These observations seem to imply that at least some of the observed regimes must be mere artifacts of a digital model, with no correspondence in a physical world. In particular, a serious problem might arise from the ubiquitous use of synchronous updating procedures for cellular systems [1,2], in which all the local states get updated in concert, since this procedure which is now applied *in physical space* can no longer be related to the use of Poincaré surface of section applicable *in phase space*. Therefore, it is important to determine to what extent and why asynchronous models of spatiotemporal dynamics are likely to differ from their synchronous counterparts.

In the present paper, we address this issue in the context of coupled map lattices. These models have been extensively studied in their synchronous form as prototypes of complex spatiotemporal dynamics. In the following section, we extend a standard version of coupled map lattices [3,5] to allow for the asynchronous updating of local states. As shown in section 3, the regimes observed in the asynchronous case are markedly different from their synchronous counterparts. The origin of these differences is investigated numerically by tuning the degree of (a)synchrony in the system. In particular, we observe that asynchrony leads to the splitting of extended coherent domains, and, under some circumstances, to the stabilization of a uniform state across the entire lattice. Stability measures are developed in section 4 to provide further insight on the effects of asynchrony on spatiotemporal dynamics. Finally, we close this paper with a brief discussion of our results in a broader context than coupled map lattices.

2. Coupled map lattices

2.1. Synchronous dynamics

Synchronous coupled map lattices are dynamical systems made of identical iterated maps interacting locally in space. One of the most common versions found in the literature is the diffusive model

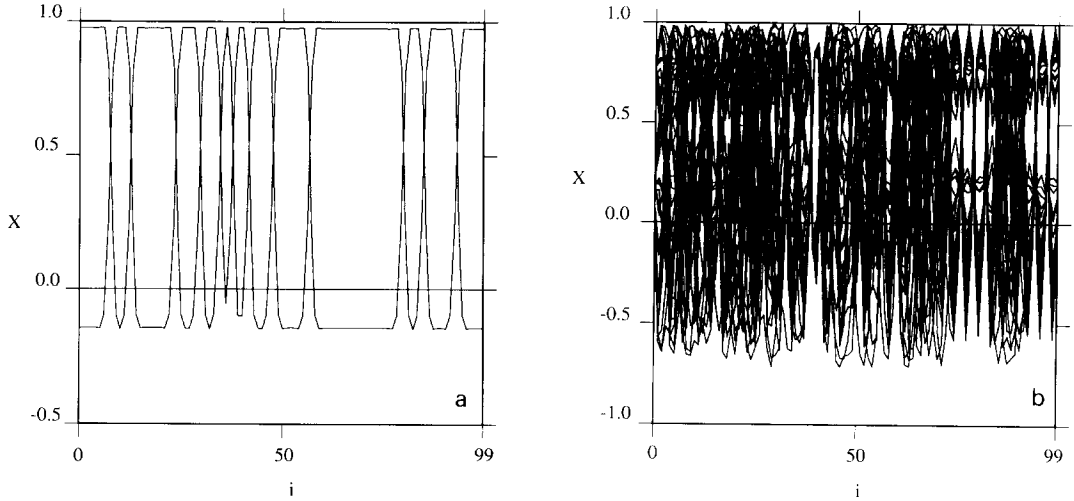


Fig. 1. Space-amplitude plots in a synchronous coupled map lattice. Amplitudes $x_i(t)$ are plotted for 50 successive time steps following the first 1000 iterations. The lattice contains 100 nodes. (a) $a = 1.2$, $\varepsilon = 0.3$. The motion is period-2 in every domain. (b) $a = 1.75$, $\varepsilon = 0.5$. Narrow chaotic domains coexist with large chaotic structures drifting in space.

$$x_i(t + 1) = (1 - \varepsilon)f(x_i(t)) + \frac{1}{2}\varepsilon\{f(x_{i-1}(t)) + f(x_{i+1}(t))\}, \quad (1)$$

where x_i is a real-valued state variable, t is a discrete time, and i designates a point in a one-dimensional lattice with N sites ($i = 1, \dots, N$). Throughout this paper, periodic boundary conditions are used. The mapping function $f(x)$ implements the local dynamics in the absence of diffusion, i.e. for a null value of the coupling constant ε . A common choice for the mapping function is the well-known logistic equation

$$f(x) = 1 - ax^2 \quad (2)$$

which exhibits a series of bifurcations leading into chaos as the parameter a is increased in the range $\{0, 2\}$. Kaneko has studied in detail the spatiotemporal regimes that appear in a coupled map lattice for a wide range of values of the parameters a and ε [5]. For small nonlinearities (i.e. $a < 1.5 \dots$), the lattice can be divided in domains of nearly uniform amplitude that have stable boundaries. In this case, the temporal motion within a domain is either periodic or chaotic, with larger domains being more unstable. For high values of the nonlinearity and a stronger diffusive coupling, the domain structure is replaced by a mixture of small chaotic regions and extended nonstationary chaotic bursts. The two types of regimes that we just described are illustrated in the space-amplitude plots of Figure 1. A detailed investigation of the regimes obtained for intermediate values of the parameters a and ε can be found in ref. [5].

2.2. Asynchronous dynamics

In order to determine what happens when asynchrony is progressively introduced in the lattice, we modify Eqs. (1) as follows. Consider a unit of time in the synchronous model – we refer to this interval in what follows as the unit of time of the original dynamics – and let us divide it into K subintervals. Taking a subinterval as the new time step, we then rewrite the lattice dynamics as

$$x_i(k+1) = P(k, K, i) \{ (1 - \varepsilon) f(x_i(k)) + \frac{1}{2} \varepsilon \{ f(x_{i-1}(k)) + f(x_{i+1}(k)) \} \} + (1 - P(k, K, i)) x_i(k), \quad (3)$$

where k is the rescaled time. $P(\cdot)$ is a boolean function defined so that each site has its state updated once every K successive subintervals. In other words, $P(k, K, i)$ must verify for all i

$$\sum_{k=t \times K}^{(t+1) \times K - 1} P(k, K, i) = 1, \quad (4)$$

where t is the original time used in Eqs. (1). The above constraint is introduced to allow for a comparison with the synchronous system of Eqs. (1). Clearly, $P(k, K, i)$ defines a model of time across the lattice, as different functional forms implement different procedures for updating local states. In what follows, we consider three such procedures, defined as

$$P(k, K, i) = \begin{cases} 1 & \text{if } (k \bmod K) = 0, \\ 0 & \text{otherwise,} \end{cases} \quad (5)$$

$$P(k, K, i) = \begin{cases} 1 & \text{if } (k \bmod K) = \text{rand}(i) \\ 0 & \text{otherwise,} \end{cases} \quad (6)$$

$$P(k, K, i) = \begin{cases} 1 & \text{if } (k \bmod K) = \text{rand}(i, k \text{ div } K) \\ 0 & \text{otherwise,} \end{cases} \quad (7)$$

where mod indicates the modulo operator and div the integer division. The expression $\text{rand}(\cdot, \cdot)$ designates a random number in the range $\{0, K - 1\}$, which depends only on the lattice site in the procedure Eq. (6), while it is also a function of the original time $t = k \text{ div } K$ in Eq. (7).

In the first procedure (i.e. Eq. (5)), all the sites in the lattice are updated synchronously, and thus Eqs. (3) are dynamically equivalent to Eqs. (1). The second procedure, defined by Eq. (6), corresponds to a phase-locked updating: each site is assigned randomly an initial time slice during which its state gets updated, and from there on, it is updated every K iterations of Eqs. (3). In the third scheme, the updating of a local state occurs once and with a uniform probability in a K -subcycle comprised between two successive time steps of the original time scale. Notice that by varying the parameter K , we can control explicitly the overall degree of asynchrony in the system. Indeed, for $K = 1$, the three procedures described above reduce trivially to the synchronous model of Eqs. (1). In the other limit of K much larger than the number of sites N , the probability of having more than one state updated in any given subcycle is negligible and the second and third procedures become analogous to what are known as the sequential and random updating schemes in Monte Carlo simulations, respectively [11]. In what follows, we will use this terminology when referring to the asynchronous updating schemes of Eqs. (6) and (7).

3. Domain breaking and temporal stabilization via asynchrony

This section summarizes the results of numerical simulations carried out in asynchronous coupled map lattices, and draws a comparison with the regimes that we described earlier in relation with a

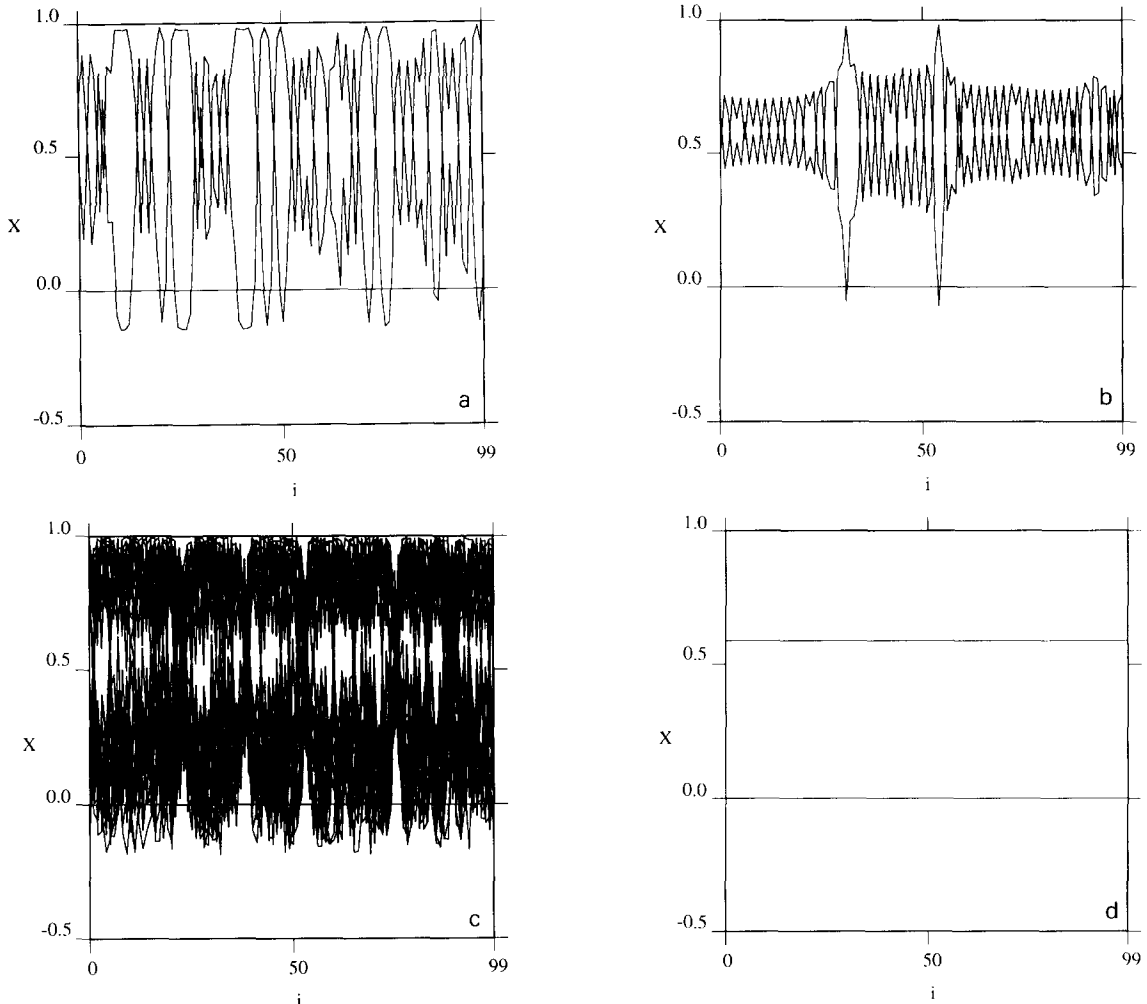


Fig. 2. Space-amplitude plots in asynchronous coupled map lattices. Amplitudes $x_i(t)$ are plotted for 50 successive time steps following the first 1000 time steps (original units of time). The lattice contains 100 nodes. (a) $a = 1.2$, $\varepsilon = 0.3$, and a sequential updating with $K = 2$ is used. Notice the splitting of large domains. (b) As in Figure 2a but with $K = 20$. Amplitudes of oscillations are reduced in this case. (c) As in Figure 2a, but with a random updating and $K = 2$. (d) As in Figure 2c, with $K = 20$. Notice the stabilization of a spatially uniform mode in this case.

synchronous model. The system, composed of $N = 100$ nodes, is first run with a parameter $a = 1.2$, a diffusive coupling coefficient $\varepsilon = 0.3$, and different degrees of asynchrony. Except for the asynchronous updating of local states, all other characteristics of the system match the synchronous model associated with Figure 1a.

Figures 2a,b depict the space-amplitude plots for 50 consecutive time steps of the original time scale, after a transient of 1000 time steps. (Each time step entails K iterations of Eqs. (3), with the amplitudes being displayed at the iterations k such that $k \bmod K = 0$). In these runs, a sequential updating was used, with a number K of subcycles equal to 2 and 20, respectively. When comparing these plots with the spatiotemporal patterns of Figure 1a, we observe drastic differences in the dynamical regimes. First, the introduction of asynchrony leads to a splitting of the large domains that were present in the synchronous case. This property is shown already on Figure 2a where $K = 2$. Increasing the degree

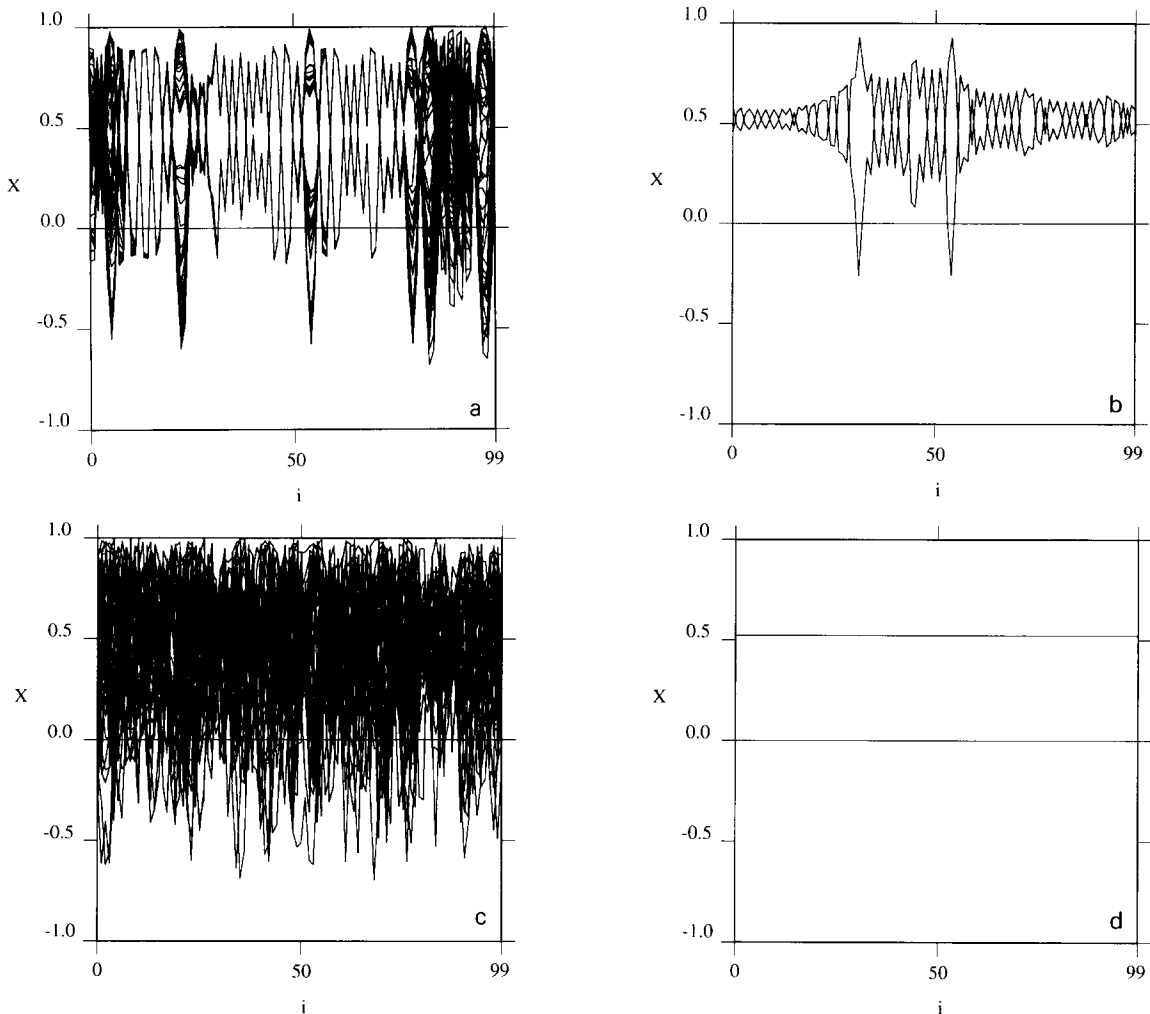


Fig. 3. Space-amplitude plots in asynchronous coupled lattices. Amplitudes $x_i(t)$ are plotted for 50 successive time steps following the first 1000 time steps (original units of time). The lattice contains 100 nodes. (a) $a = 1.75$, $\varepsilon = 0.5$, and a sequential updating with $K = 2$ is used. (b) As in Figure 3a but with $K=20$. (c) As in Figure 3a, but with a random updating and $K = 2$. (d) Random updating with $K = 20$.

of asynchrony from $K = 2$ to $K = 20$ produces a contraction of the local amplitudes of oscillations, as illustrated in Figure 2b. Similar remarks can be made when observing the regimes derived from a random updating of states, as shown in Figures 2c,d. Notice that the complex dynamics associated with random updatings leads to a localization of local states around the fixed point of the logistic map. This trend is reinforced with further increases of K .

The above runs were repeated for the values of a and ε used in the synchronous simulation of Figure 1b, namely $a = 1.75$ and $\varepsilon = 0.5$. Again, introducing asynchrony produces the breaking of large spatiotemporal patterns into smaller structures (Figures 3a and c). When more temporal slices in which states may be updated are introduced (i.e. for $K=20$), we observe a dramatic simplification of the local temporal dynamics with respect to the synchronous case. While sequential updatings lead to a quasi-periodic motion of period-2 (cf. Figure 3b), random updatings produce a complete stabilization

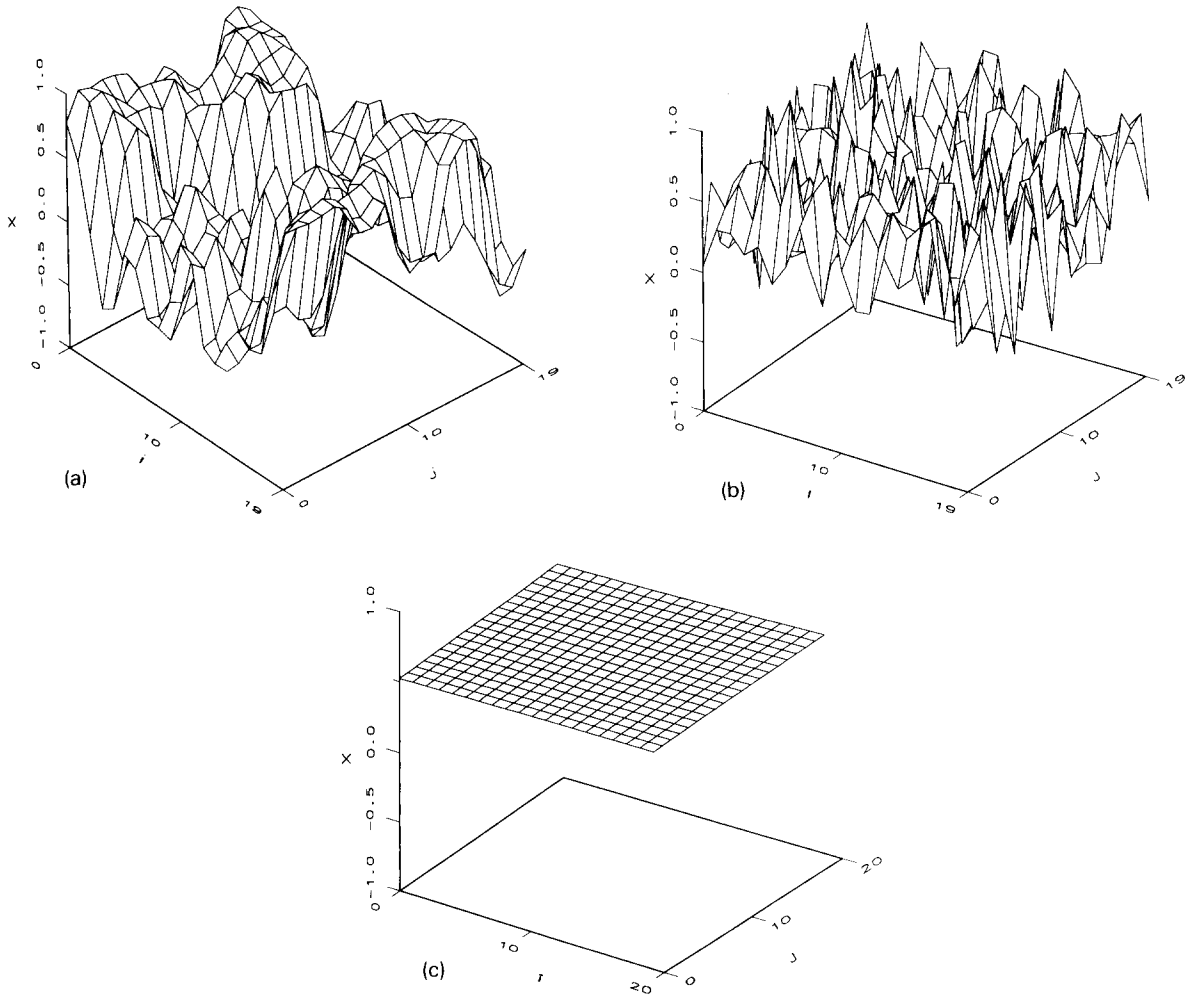


Fig. 4. Space-amplitude plots for a two-dimensional coupled lattice. Amplitudes $x_i(t)$ are plotted after 1000 time steps (original units of time). The lattice contains 20×20 nodes. (a) $a = 1.75$, $\varepsilon = 0.5$, and a synchronous updating is used. (b) As in Figure 4a but using a random updating with $K = 2$. (c) Random updating with $K = 20$.

of the system, as shown in Figure 3d. The very same qualitative characteristics are also found in a two-dimensional lattice with diffusive coupling to nearest neighbors, as shown in Figures 4. The model comprises a 20×20 lattice, with $a = 1.75$ and $\varepsilon = 0.5$. Figure 4a displays a space-amplitude plot after 1000 iterations of the synchronous model. Similar plots are given in Figure 4b,c, for a model based on random updatings, and a number of subcycles K equal to 2 and 20, respectively.

In conclusion, asynchronous spatiotemporal regimes in coupled map lattices are markedly different from their corresponding synchronous regimes. When asynchrony is fully developed, these differences translate into an enhanced stability of the local dynamics. A precursor of the enhanced stability seems to be the breakup of large spatial domains into smaller structures, thus suppressing long-range coherence in the lattice. These signatures of asynchrony are found both with sequential and a random updating schemes, despite the different nature of the associated dynamical systems: one (i.e. the sequential model) is deterministic while the other is stochastic. Notice also that the signatures of asynchrony

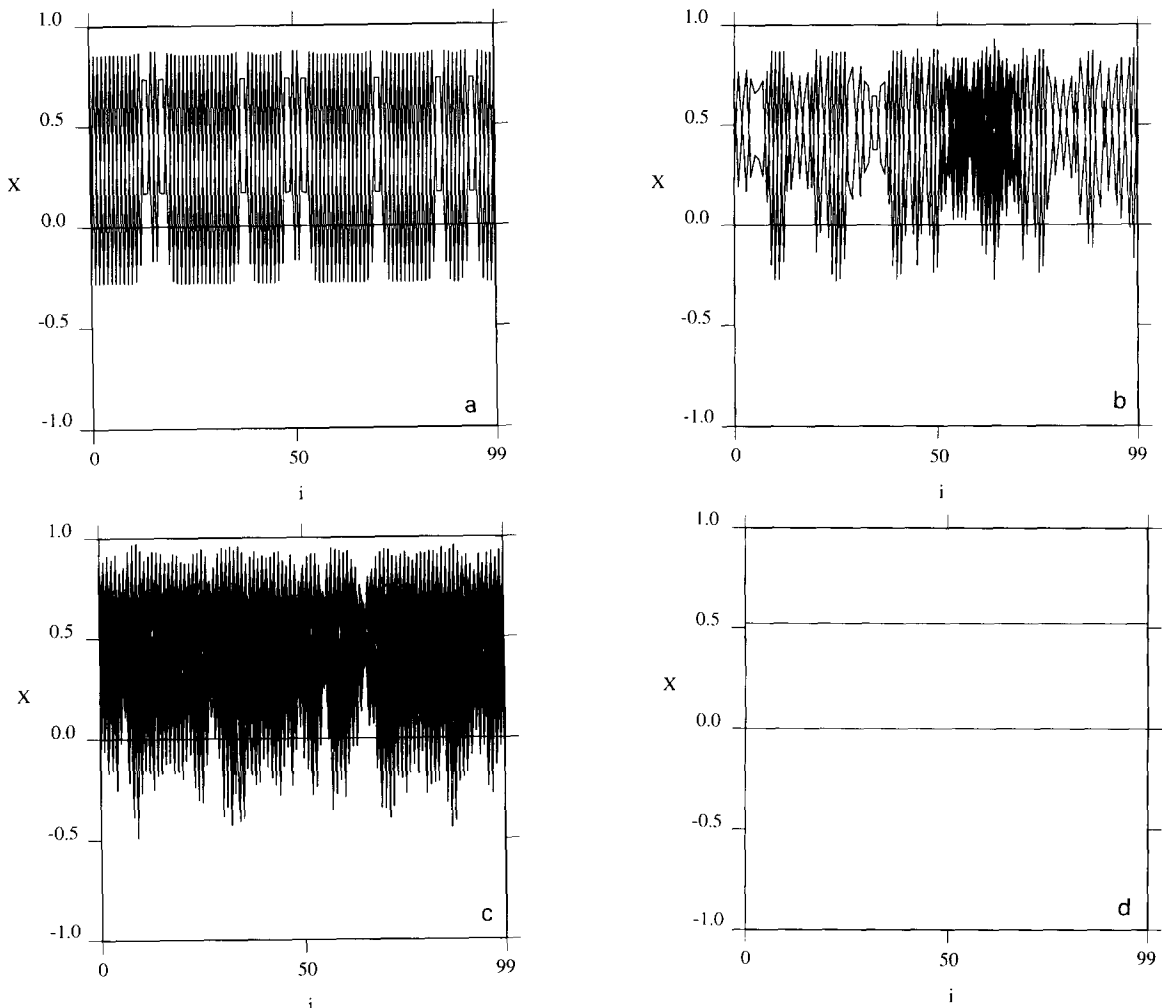


Fig. 5. Space-amplitude plots in lattices with linear coupling. Amplitudes $x_i(t)$ are plotted for 50 successive time steps following the first 1000 time steps (original units of time). The lattice contains 100 nodes. (a) $a = 1.75$, $\varepsilon = 0.5$, and synchronous updating. (b) As in Figure 5a but using a sequential updating instead, with $K = 2$. (c) Random updating with $K = 2$. (d) Sequential or random updating with $K = 20$

are robust to changes in the functional form of the diffusive coupling term in Eqs. (1) and (3). For instance, similar characteristic patterns are found when a linear coupling among local state variables replaces the nonlinear $f(x)$ -coupling form, as demonstrated in Figures 5a-d. In the following section, we rely on simple notions of stability to explain qualitatively these dynamical signatures of asynchrony.

A final point is in order. Asynchronous coupled map lattices are expected to exhibit a rich set of complex spatiotemporal patterns just as their synchronous counterparts do, as the model parameters a , ε , and K are varied. A detailed investigation of these regimes and their location in a continuous phase diagram is beyond the scope of this paper. Such a study will be developed elsewhere. For now, suffice it to note that the typical domain sizes tend to decrease as the degree of asynchrony K is increased in the regions of phase-space probed by Figures 2 and 3. The coherent domains are fixed in time in these cases. Notice also the coexistence for these parameter values of a large number of attractors

corresponding to different domain structures, which are reached from different initial conditions. For intermediary coupling strengths, say $\epsilon = 0.3$, and a nonlinearity $a = 1.75$, the dependency of domain sizes on the value of K is preserved, but the domain boundaries move slowly across the lattice. Finally, remarkable regimes observed with synchronous models [5], such as the motion of localized chaotic defects through quasiperiodic zigzag regions, are found in asynchronous models, for instance with parameters $a = 1.8$, $\epsilon = 0.1$, $K = 2$, and a sequential updating scheme. However, the mixing of iterates of different order induced by the sequential procedure – this is a fundamental consequence of asynchrony and thus, of spatial extension, as we will show below - translates into the invasion of zigzag regions by large chaotic defects.

4. Asynchronous mixing of states

Numerical simulations of asynchronous coupled map lattices revealed a characteristic breakup of large spatial domains, and, for high degrees of asynchrony, the enhanced stability of simple spatiotemporal regimes. Let us first consider here the splitting of extended domains. To this end, we suppose that the system is started in a spatially uniform state, so that $x_i(0) = x^0$ at all the sites i in the lattice. Note that one could consider instead a spatial domain that is large enough so that boundary effects can be neglected. As can be readily seen from Eqs. (1), a synchronous evolution of states will maintain a spatial uniformity ad infinitum. Thus, the system reduces to a single degree of freedom, namely the uniform state $x(t)$, which evolves in time according to the nonlinear mapping $x(t + 1) = f(x(t))$. This locked evolution accepts the following pictorial representation:

$$\begin{matrix} x_1(0) = x^0 & \rightarrow & x_1(1) = f(x^0) & \rightarrow & \dots \\ \vdots & & \vdots & & \vdots \\ x_N(0) = x^0 & \rightarrow & x_N(1) = f(x^0) & \rightarrow & \dots \end{matrix}$$

which we contrast with a fully sequential updating of states such that the sequence of updates follows the numbering of sites in the lattice. Assuming for simplicity that each site is only coupled to its left neighbor, the sequential dynamics unfolds in space and time as:

$$\begin{matrix} x_1(0) = x^0 & \rightarrow & x_1(1) = (1 - \epsilon)f(x^0) + \epsilon f(x_N(0)) & = & f(x^0) & \rightarrow & \dots \\ x_2(0) = x^0 & \rightarrow & x_2(1) = (1 - \epsilon)f(x^0) + \epsilon f(x_1(1)) & & & \rightarrow & \dots \\ \vdots & & \vdots & & \vdots & & \\ x_N(0) = x^0 & \rightarrow & x_N(1) = (1 - \epsilon)f(x^0) + \epsilon f(x_{N-1}(1)) & & & \rightarrow & \dots \end{matrix}$$

where the time t is expressed in the units of the synchronous dynamics. It is easy to convince oneself from this representation that the asynchronous updating of local states combined with their diffusive coupling introduces a mixing of successive iterations of the logistic map. This leads to a progressive collapse of the uniform spatial amplitude and thus the splitting of coherent domains. Given the particular sequence of updates which is used in the sequential procedure, there is a natural mapping from space (i.e. a position in the lattice) to time (i.e. an iteration number) which allows us to rewrite the asynchronous lattice dynamics in terms of a single variable and a higher-order iterated map as

$$x(k) = (1 - \epsilon)f(x(k - N)) + \epsilon f(x(k - 1)), \quad k \geq N \tag{8}$$

with the time $t = k \operatorname{div} N$ and the position in the lattice $i = k \operatorname{mod} N + 1$.

In the trivial case of a lattice with two sites, the above equation reduces to

$$x(k) = (1 - \varepsilon)f(x(k - 2)) + \varepsilon f(x(k - 1)), \quad k \geq 2 \tag{9}$$

which is an iterated map of the second order. Comparing the dynamical properties of this map with those of the simple logistic map is quite enlightening with regard to features of asynchronous dynamics exhibited in the previous section. This analysis will be reported elsewhere.

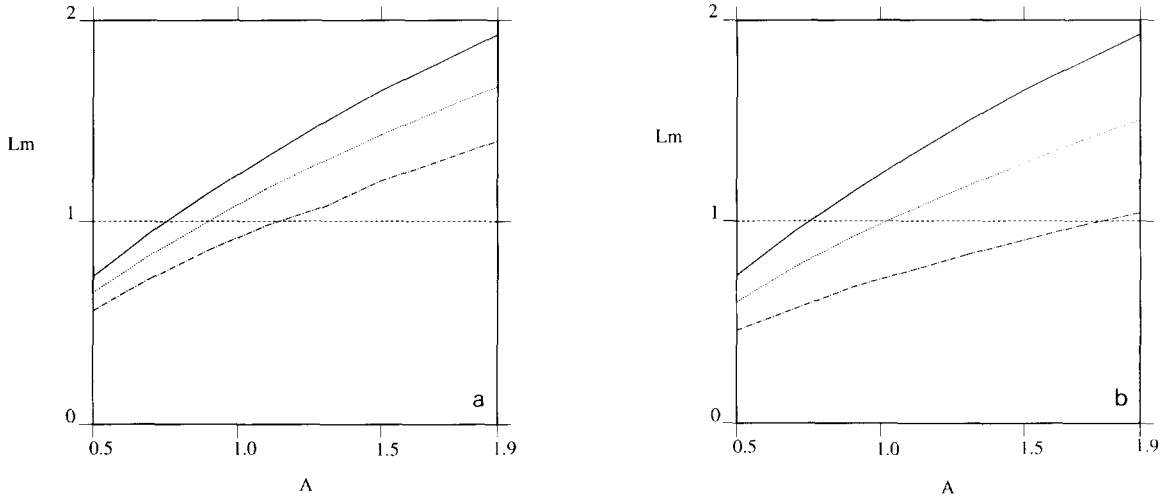
For now, we will take a more quantitative approach to explain the enhanced stability in asynchronous systems with respect to their synchronous counterpart, by restricting ourselves to perturbations in the vicinity of spatially homogeneous regimes. Consider first the synchronous model of Eqs. (1). This system admits a uniform solution $x_i = x^*$ for all i , which is stable whenever the Jacobian matrix of the system computed around the homogeneous state has all its eigenvalues inferior to 1 in absolute value. (x^* is the fixed point of the logistic map). For a lattice made of N nodes, the $N \times N$ Jacobian matrix, J_{sync} is tridiagonal, and reads as

$$J_{\text{sync}} = -2ax^* \begin{pmatrix} 1 - \varepsilon & \varepsilon/2 & 0 & \cdots & \varepsilon/2 \\ \varepsilon/2 & 1 - \varepsilon & \ddots & \ddots & \vdots \\ 0 & \ddots & \ddots & \ddots & 0 \\ \vdots & \ddots & \ddots & 1 - \varepsilon & \varepsilon/2 \\ \varepsilon/2 & \cdots & 0 & \varepsilon/2 & 1 - \varepsilon \end{pmatrix}. \tag{10}$$

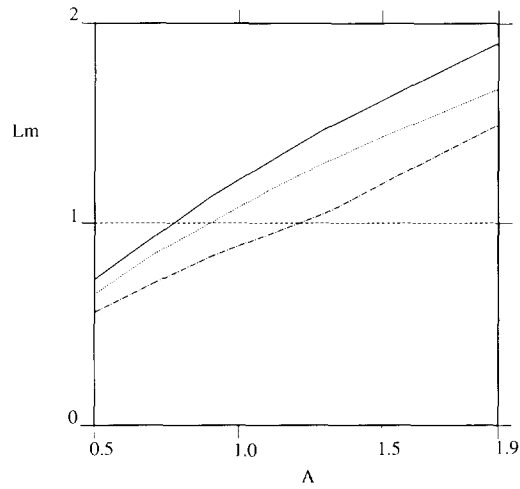
Let us consider again a partially sequential updating of states (i.e. with $K < N$). When the sequence of updates follows the numbering of sites in the lattice, an equivalent Jacobian matrix, J_{seq} , may be defined as the product of the Jacobians computed from Eqs. (3) for K successive updating cycles. Each matrix in this product has a number of rows that are identical to those of the synchronous Jacobian, and which correspond to the nodes being updated during the associated iteration. The rest of the matrix is diagonal, with the diagonal elements equal to one. Stated more formally, we have

$$J_{\text{seq}} = \begin{pmatrix} 1 & 0 & \cdots & \cdots & 0 \\ 0 & 1 & \ddots & & \vdots \\ \vdots & \ddots & \ddots & \ddots & \vdots \\ 0 & \cdots & 0 & 1 & 0 & \cdots & 0 \\ J_{\text{sync}}^{m1} & \cdots & \cdots & \cdots & J_{\text{sync}}^{mN} \\ \vdots & \cdots & \cdots & \cdots & \vdots \\ J_{\text{sync}}^{N1} & \cdots & \cdots & \cdots & J_{\text{sync}}^{NN} \end{pmatrix} \underbrace{\begin{pmatrix} \cdots \\ \cdots \\ \cdots \end{pmatrix}}_{K-2} \begin{pmatrix} J_{\text{sync}}^{11} & \cdots & \cdots & \cdots & J_{\text{sync}}^{1N} \\ \vdots & \cdots & \cdots & \cdots & \vdots \\ J_{\text{sync}}^{m1} & \cdots & \cdots & \cdots & J_{\text{sync}}^{mN} \\ 0 & \cdots & 0 & 1 & 0 & \cdots & 0 \\ \vdots & \cdots & \ddots & \ddots & \ddots & \ddots & \vdots \\ \vdots & \cdots & \cdots & \ddots & \ddots & \ddots & 0 \\ 0 & \cdots & \cdots & \cdots & 0 & 1 \end{pmatrix}. \tag{11}$$

where m verifies the relation $N = mK$. The above considerations of linear stability do not apply rigorously in the case of random updatings, for one is dealing then with a stochastic model. Nevertheless, it is useful to introduce an equivalent jacobian matrix, J_{rand} , defined over any given sequence of K successive updatings that make for a unit of time of the synchronous dynamics. As for J_{seq} , the matrix J_{rand} is written as the product of K Jacobians computed from Eqs. (3). Each matrix in this



— sync seq,k=20 - - - - rand,k=20 ref — sync seq,k=20 - - - - rand,k=20 ref
 Fig. 6. Maximum eigenvalue of the Jacobian in absolute value vs. the parameter of nonlinearity, a , for synchronous and asynchronous dynamics. The lattice contains 50 nodes. (a) $\epsilon = 0.3$. (b) $\epsilon = 0.5$



— seq,k=5 seq,k=20 - - - - seq,k=50 ref
 Fig. 7. Maximum eigenvalue of the Jacobian in absolute value vs. the parameter of nonlinearity, a , for increasing degrees of asynchrony using sequential updatings. The lattice contains 50 nodes and the coupling $\epsilon = 0.3$.

product has a number of rows that are identical to those of the synchronous Jacobian, and which correspond to the nodes being updated during the associated iteration. The remaining rows are diagonal, with the diagonal elements equal to one. Given the stochastic sequencing of updates in the random scheme, each series of K successive updates produces a different matrix J_{rand} . Thus, in what follows, we consider average properties over ensembles of such matrices.

In order to compare the stability of the synchronous and asynchronous models, we have computed numerically the largest eigenvalue in absolute value in the matrices J_{sync} , J_{seq} , and J_{rand} ^{#1} as a function of the parameter a , in a system with $N = 50$ sites. As shown in Figure 6a, the spatially uniform mode becomes unstable for values of the parameter a that are larger in the asynchronous systems than in the synchronous lattice. Furthermore, Figure 6b shows that this trend is accentuated for stronger diffusive couplings. Notice also that stability is strongest in asynchronous models using a random updating scheme. Finally, Figure 7 shows that the threshold of instability increases with the degree of asynchrony, as defined by the parameter K . Thus, the linear stability analysis in the vicinity of a spatially uniform mode confirms that asynchrony tends to stabilize this regime. By extrapolation, the analysis also suggests that higher-order spatiotemporal modes that are unstable in a synchronous model might be stable in the corresponding asynchronous model. These results are consistent with the empirical findings of the previous section, even though the size of the lattice used in this section was reduced by half for practical reasons. (Compare for instance the period-2 oscillations in Figure 3b with the complex synchronous dynamics of Figure 1b. In addition, the fixed point regime in Figure 3d can be related to the unstable crossover of the corresponding Lyapunov exponent in Figure 6b). To close, let us emphasize that we have only considered here the temporal stability of a uniform mode. However, earlier studies have shown that its spatial stability will typically be lost as well when one is at a sufficient distance above the critical threshold of temporal instability [14], due to the nonlinear coupling with modes of higher spatial frequency.

5. Conclusion

The idea of reducing the study of continuous time systems to that of an associated discrete time system was first proposed by Poincaré. While applicable to low-order dynamical systems (i.e. represented by a finite set of ordinary differential equations), the discretization of time raises new questions in the case of extended systems in which, in addition, a finite discretization in space has been performed. In this paper, we have illustrated this problem by unraveling the striking disparities existing between synchronous and asynchronous spatiotemporal dynamics in coupled map lattices. Given these disparities, it is not clear to what extent synchronous models of spatiotemporal chaos provide reliable descriptions of real phenomena. The signatures of asynchrony in coupled map lattices, namely the splitting of extended homogeneous domains mediated by the mixing of successive iterates of neighbor state variables, and in some circumstances, the stabilization of a uniform state across the entire lattice, might be found in other spatially distributed systems. For instance, simulations of evolutionary games taking place on a two-dimensional grid of the kind first studied in [13] exhibited very similar patterns when updates of states were made asynchronously [12]. More work is clearly needed in the future in order to better characterize the spatiotemporal regimes produced by asynchronous models of extended systems such as those considered in this paper, in particular under parametric conditions that do not translate into a global fixed point. Ultimately, this effort might lead to a deeper understanding of complex dynamics in spatially distributed systems.

^{#1} For the largest eigenvalue of J_{rand} , averages are taken over 5 sample Jacobian matrices. Deviations from the mean are verified to be within a 1–2 percent range. The property of a maximum absolute eigenvalue being either inferior or superior to 1 is verified to hold for Jacobians defined over several time units.

Acknowledgements

This research was supported in part by the Belgian government under the Pôles d'Attraction Interuniversitaires and by a grant from Zetes Electronics.

References

- [1] S. Wolfram, ed., *Theory and Applications of Cellular Automata* (World Scientific, Singapore, 1986).
- [2] H. Gutowitz, ed., *Cellular Automata: Theory and Experiment*, *Physica D* 45 (1990).
- [3] K. Kaneko, *Prog. Theor. Phys.* 72 (1984) 480.
- [4] R. Kapral, *Phys. Rev. A* 31 (1985) 3868.
- [5] K. Kaneko, *Physica D* 34 (1989) 1.
- [6] H. Poincaré, *Les Méthodes Nouvelles de la Mécanique céleste* (Gautier-Villars, Paris, 1899).
- [7] D.T. Gillespie, *J. Comput. Phys.* 22 (1976) 403.
- [8] H.A. Cecatto, *Phys. Rev. B* 37 (1986) 4734.
- [9] R. Thomas, *J. Theor. Biol.* 42(1973) 563.
- [10] R. Thomas and R. D'Ari, *Biological Feedback* (CRC Press, Boca Raton, 1990).
- [11] D.T. Gillespie, *Markov Processes: An Introduction for Physical Scientists* (Academic Press, 1992).
- [12] B.A. Huberman and N. Glance, preprint, 1993.
- [13] M.A. Nowak and R.M. May, *Nature* 359 (1992) 826.
- [14] C. Nicolis, G. Nicolis and Q. Wang, *Int. J. Bifurc. Chaos* 2 (1992) 263.